Journal of the Optical Society of America B
OPTICAL PHYSICS

Spectroscopic study of the $4f^7 6s^2\ {}^8S^\circ_{7/2} - 4f^7({}^8S^\circ)6s6p({}^1P^\circ)\ {}^8P_{9/2}$ transition in neutral europium-151 and europium-153: absolute frequency and hyperfine structure

M. T. Herd,[1] C. Maruko,[2] M. M. Herzog,[2] A. Brand,[2] G. Cannon,[1] B. Duah,[2] N. Hollin,[2] T. Karani,[2] A. Wallace,[2] M. Whitmore,[2] and W. D. Williams[2,*]

[1]Department of Biological and Physical Sciences, Assumption University, Worcester, Massachusetts 01609, USA
[2]Department of Physics, Smith College, 44 College Lane, Northampton, Massachusetts 01063, USA
*Corresponding author: wwilliams@smith.edu

Received 16 June 2022; revised 19 August 2022; accepted 22 August 2022; posted 22 August 2022; published 9 September 2022

We report on spectroscopic measurements on the $4f^7 6s^2\ {}^8S^\circ_{7/2} \rightarrow 4f^7({}^8S^\circ)6s6p({}^1P^\circ)\ {}^8P_{9/2}$ transition in neutral europium-151 and europium-153 at 459.4 nm. The center of gravity frequencies for the 151 and 153 isotopes, reported for the first time in this paper, to our knowledge, were found to be 652,389,757.16(34) MHz and 652,386,593.2(5) MHz, respectively. The hyperfine coefficients for the $6s6p({}^1P^\circ)\ {}^8P_{9/2}$ state were found to be A(151) = −228.84(2) MHz, B(151) = 226.9(5) MHz and A(153) = −101.87(6) MHz, B(153) = 575.4(1.5) MHz, which all agree with previously published results except for A(153), which shows a small discrepancy. The isotope shift is found to be 3163.8(6) MHz, which also has a discrepancy with previously published results.

https://doi.org/10.1364/JOSAB.467968

1. INTRODUCTION

Europium has two stable isotopes: europium-151 and europium-153. The two isotopes have natural abundances of 47.8% and 52.2%, respectively. Properties of the excited and ground states of europium such as hyperfine structure, isotope shifts between the two stable isotopes, and excited state lifetimes have been extensively studied. The absolute transition frequency between the ground state and the $4f^7({}^8S^\circ)6s6p({}^1P^\circ)\ {}^8P_{9/2}$ state is the subject of investigation in this work. It was first measured by Russell and King in 1939 who collected light emitted from an arc lamp. [1] To the best of our knowledge, the last measurement of the absolute frequency was measured in 1983 by Smith and Tomkins [2]. However, the reported value of 21,761.30(2) cm^{-1}(652,387,360(600) MHz) was with respect to the Doppler broadened spectrum that, due to unresolved hyperfine structure and overlapping spectrum from the two stable isotopes, had a width 0.2 cm^{-1}(6,000 MHz). Therefore, the transition frequency for the center of gravity for each isotope has yet to be measured to high precision. For the remainder of this paper, we will refer to the excited state using the shortened, historical designation of $y\ {}^8P_{9/2}$.

In 2020, Furmann *et al.* performed laser induced fluorescence spectroscopy on europium and obtained magnetic dipole constants and electric quadrupole constants of 26 electronics levels, ranging between 28000 cm^{-1}−40000 cm^{-1} [3]. In that work, Furmann *et al.* also compiled hyperfine coefficients and isotope shifts for a large number of states for the two stable isotopes.

In the past few years, there has been renewed interest in europium and in the $y\ {}^8P_{9/2}$ state. Spectroscopic work has been done on the $y\ {}^8P_{9/2}$ state to find the branching ratios from that state [4]. The $y\ {}^8P_{9/2}$ state was then used as part of a laser cooling and trapping scheme to create a magneto-optical trap of ultracold europium [5,6] and used to populate lower lying metastable states to study one-body losses in magnetically trapped metastable europium [7]. Finally, the first europium Bose–Einstein condensate (BEC) was successfully created in 2022 [8] and a proposal to create dual species rubidium and europium BEC was recently published [9].

Simplified Grotrian diagrams for the two stable isotopes are shown in Fig. 1. The relative intensities of the hyperfine transitions can be found using the formula

$$I_r = (2F+1)(2F'+1)\begin{Bmatrix} J & I & F \\ F' & 1 & J' \end{Bmatrix}^2, \tag{1}$$

where $J = 7/2$ and F are the total electronic angular momentum and total atomic angular momentum for the ground state, respectively, $J' = 9/2$ and F' are for the $y\ {}^8P_{9/2}$ state, and $I = 5/2$ is the nuclear spin for both isotopes. The

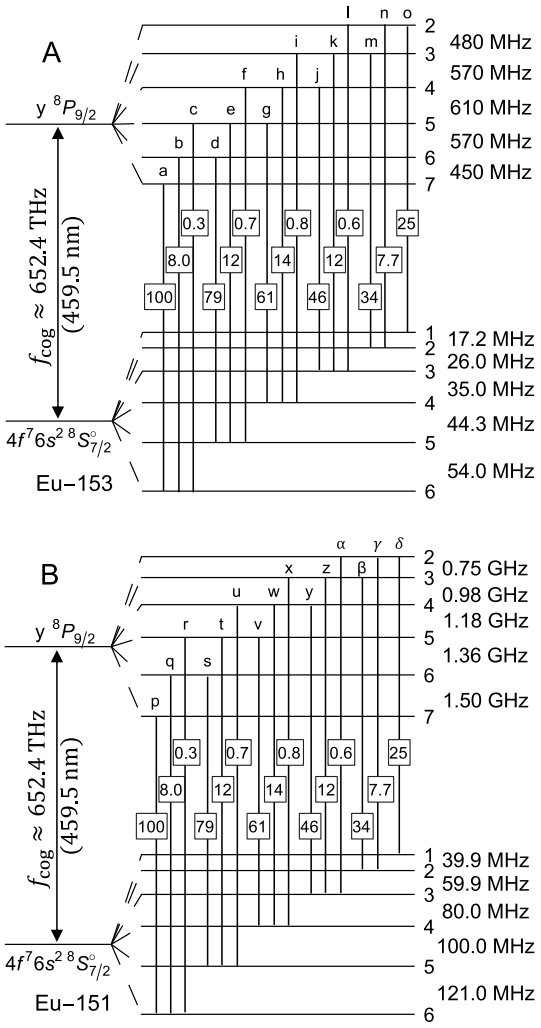

Fig. 1. Simplified Grotrian diagrams for (A) europium-153 and (B) -151. The boxed values represent the relative intensities of the allowed transitions, normalized to the strongest transition.

$F = 6 \rightarrow F' = 7$ transition is the largest intensity transition, and can be used to normalize the intensity of the other transitions. The normalized values are the boxed values in Fig. 1.

Both stable isotopes of europium possess equal values of the nuclear spin $I = 5/2$, which causes hyperfine splittings in both the ground state and excited states. The hyperfine splitting from the center of gravity of a state is given by

$$\frac{1}{2}AK + B\frac{(3/2)K(K+1) - 2I(I+1)J(J+1))}{2I(2I-1)2J(2J-1)}, \quad \textbf{(2)}$$

where $K = F(F+1) - I(I+1) - J(J+1)$, A is the magnetic dipole constant, B is the electric quadrupole constant, I is the nuclear spin, J is the total electronic angular momentum, and F is the total atomic angular momentum. There are higher order terms for Eq. (2), for example, a term for the magnetic octupole constant C, which is not shown since it is beyond the precision of this work. The most precise value for the hyperfine constants of the ground state were measured by Sanders *et al.* with values A(151) = −20.0523(2) MHz, B(151) = −0.7012(35) MHz, A(153) = −8.8532(2) MHz, and B(153) = −1.7852(35) MHz [10]. The hyperfine coefficients for the $y\ ^8P_{9/2}$ state were measured by Zaal *et al.* with values A(151) = −228.9(2) MHz, B(151) = 226(4) MHz, A(153) = −102.4(2) MHz, and B(153) = 575(8) MHz [11].

In this work, saturated absorption spectroscopy was performed between the ground state and the $y\ ^8P_{9/2}$ state in neutral europium-151 and europium-153. The paper is organized as follows: Section 2 gives an overview of the experimental setup, Section 3 presents data, a discussion of systematic effects, and the final results, and Section 4 summarizes the results of this work and discusses possible future improvements to determine the center of gravity frequencies to higher precision.

2. EXPERIMENTAL SETUP

The experimental design is composed of two main components: a double pass acousto-optic modulator (AOM) setup to stabilize and scan the laser frequency with respect to a frequency comb and a saturated absorption spectroscopy setup for the europium atoms. The experimental setup to stabilize, measure, and control the frequency of the laser is shown in Fig. 2. A titanium sapphire laser (MSquared SOLSTIS) is used to produce 919 nm light. Most of the light is sent to a frequency doubling cavity (MSquared ECD-X), which is then fiber coupled to the saturated absorption setup. A small portion of the 919 nm light is sent to a double pass AOM (Brimrose GPM-800-200) setup [12]. The AOM has a center frequency of 800 MHz and a measured double pass bandwidth of ∼225 MHz. The frequency of the light after the double pass AOM is given by $f_{l,IR} + 2f_{\mathrm{AOM}}$, where $f_{l,IR}$ is the frequency of the laser leaving the titanium sapphire laser, and f_{AOM} is the frequency driving the AOM. This particular AOM is efficient with only horizontally polarized light. As such, a 90/10 non-polarizing beam splitter is used in place of a traditional polarizing beam splitter and quarter-wave plate. This experimental arraignment loses 90% of the incoming light but sends 90% of the doubly diffracted light to a fiber coupler. Before entering the AOM, there is 1.5 mW of laser light. Before the fiber coupler, there is between 40 μW and 100 μW of laser power, depending upon the frequency driving the AOM. The doubly diffracted light is then amplified (ThorLabs BOA930S) and power stabilized (Thorlabs EVOA800F) to 1.5 mW before being sent to both a wavemeter (High-Finesse/Angstrom WS7-30) and frequency comb (Toptica DFC). This arrangement keeps a constant 1.5 mW of laser power being sent to the wavemeter and frequency comb independent of f_{AOM}. The frequency comb, which has a repetition rate of $f_{\mathrm{rep}} = 80$ MHz, is calibrated to a GPS-referenced atomic clock (Stanford Research Systems FS740). The function generator driving the double pass AOM (Stanford Research Systems SG384) is also referenced to the atomic clock. The wavemeter is used to determine the frequency comb mode number. The doubly diffracted light is beat against the frequency comb and stabilized using a proportional–integral–derivative (PID) controller (Toptica DigiLock) so that the laser is 20 MHz above a specified frequency comb mode. With the PID controller activated, the frequency of the doubly diffracted light is fixed according to the equation

$$f_{l,IR} + 2f_{\mathrm{AOM}} = n(80\ \mathrm{MHz}) + 20\ \mathrm{MHz}, \quad \textbf{(3)}$$

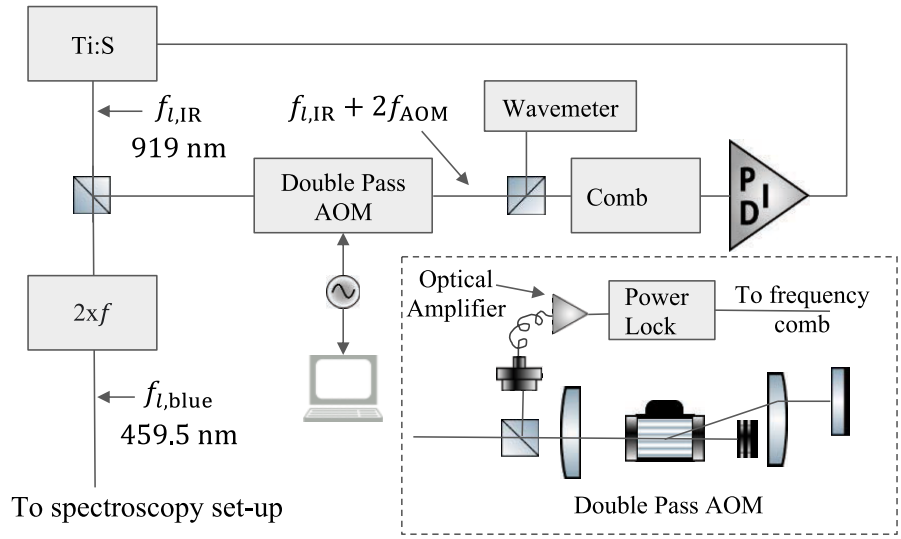

Fig. 2. Simplified experimental setup to stabilize, measure, and control the frequency of the laser. See text for details.

where n is the frequency comb mode number, 80 MHz is the repetition rate of the frequency comb, and +20 MHz is the positive beat note. The right-hand side of this equation is a constant, so smoothly scanning the frequency driving the AOM results in the laser frequency changing to keep the left-hand side of Eq. (3) equal to the right-hand side. This experimental setup allows the scanning of the laser frequency (in the infrared) by over 650 MHz to a precision of better than 1.5 kHz.

The rest of the infrared light is sent through a frequency doubling cavity before being fiber coupled to the saturated absorption setup; see Fig. 3. The waist of the laser leaving the fiber coupler is approximately 2 mm. A half-wave plate and polarizing beam splitter are used to control the power of the probe beam. The pump beam passes through an AOM (ISOMET M1201-SF40-1.7) that is driven at 40 MHz. The frequency driving the AOM is chopped at 27.13 kHz for demodulation using the first harmonic by a lock-in amplifier (Standford Research Systems SR830 DSP); the function generator (Stanford Research Systems SG382) driving this AOM is also referenced to the atomic clock. The diffracted pump beam's power is controlled by a second half-wave plate and polarizing beam splitter.

The diffracted pump beam and probe beam counterpropogate through a home-built hollow cathode lamp. The lamp, which is modeled after the work of Sulai *et al.* [13] and Saini *et al.* [14], is composed of hollow electrodes: a cathode held at a negative voltage and two grounded anodes. The anodes are made of stainless steel and have an outer diameter of 16.5 mm, inner diameter of 6.35 mm, and length of 3.8 mm. The cathode is also made from stainless steel with an outer diameter of 16.5 mm, inner diameter of 7.1 mm, and length of 10.4 mm. A hollow cylinder made from europium (American Elements EU-M-02RM-TU) with an outer diameter of 7 mm, inner diameter of 6 mm, and length of 10 mm is placed in the cathode. Two thin stainless steel end caps are used to secure the europium in the electrode. There is 4.45 mm between the edge of the cathode and the nearest edge of an anode.

The lamp is filled with argon gas varying in pressure from 100 mTorr to 500 mTorr and driven with currents ranging from −3 mA to −20 mA. When in constant current mode, the voltages across the lamp varied between −150 V and −400 V depending upon the current and pressure of the argon gas. The power supply (KEPCO BOP 500 M) used for this experiment can be run in constant current or constant voltage mode. Constant current mode was used for most studies; constant voltage mode was used to look for energy level shifts due to the applied external voltage. We found the lamp runs in three possible modes. The first mode consists of the discharge mostly outside the electrodes, producing very weak signals. This is expected since the laser light travels through the center of the electrodes. The second mode has the discharge mostly contained within the electrode, but additional plasma outside. Once the second mode is present, the discharge slowly concentrates inside the electrode. The fully concentrated plasma we call the third mode. If we monitor an atomic signal, the subDoppler features become larger and larger as the lamp moves from the second mode to the third mode. The voltage needed to drive the lamp in constant current mode also slowly becomes less negative from the second mode to the third mode. We monitor the voltage of the power supply until it reaches a steady state (fully in the third mode) before collecting data. The powers of the diffracted pump beam and probe beam were measured before each data run using photodetectors (Thorlabs PDA36A2); the voltage outputs of the photodetectors were calibrated to laser power using a power meter (Thorlabs PM100D). Finally, the transmission of the probe beam was monitored using a photodetector (Thorlabs PDA36A2). The output of this photodetector was demodulated by the lock-in amplifier. The output of the lock-in amplifier was recorded by a computer along with the frequency driving the double pass AOM from Fig. 2.

The frequency of the probe beam interacting with the atoms is given by the equation

$$f_{l,\mathrm{blue}} = 2\,f_{l,IR} = 2(n(80\ \mathrm{MHz}) + 20\ \mathrm{MHz} - 2\,f_{\mathrm{AOM}}). \quad \textbf{(4)}$$

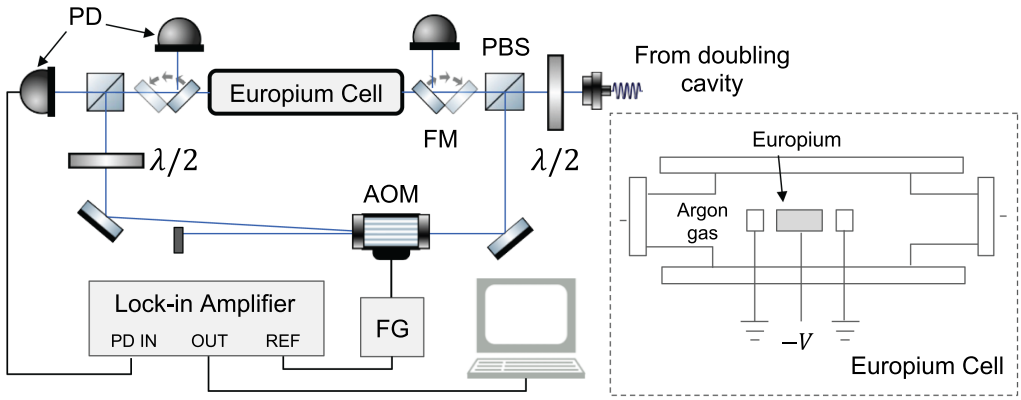

Fig. 3. Saturated absorption setup. λ/2, half-wave plate; PBS, polarizing beam splitter; FM, flip mirror; PD, photodetector; AOM, acousto-optic modulator; FG, function generator.

The pump beam has a frequency that is 40 MHz larger than the probe beam, so the resultant spectrum will be shifted 20 MHz lower than the actual zero Kelvin spectrum. The uncertainty on the frequency of the light for the pump beam and the probe beam is better than 3 kHz.

3. RESULTS

Data are collected by scanning the frequency driving the double pass AOM between 635 MHz and 965 MHz, or equivalently scanning the frequency of the laser probing the atoms by 1320 MHz. The spectrum (see Fig. 4) is approximately 8 GHz wide requiring multiple regions of data collection. The centers of the regions are separated by 1280 MHz, which is equivalent to moving eight frequency comb mode numbers. Each region has an overlap of 40 MHz. The data are then stitched together before fitting.

As can be seen in Fig. 4, the spectra from the two isotopes overlap each another. The lower frequency range of the spectrum is due mostly to transitions and crossovers from the europium-153 isotope. It should be noted that while some of the features look like derivative signals, the combination of negative and positive Lorentzian features only gives the appearance of derivative signals; the pump beam is amplitude modulated. Due to the large number of hyperfine states and transitions

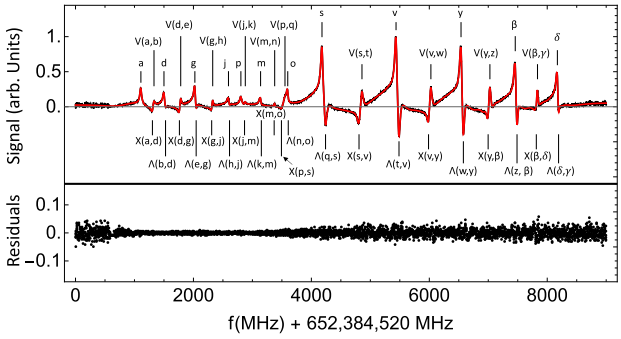

Fig. 4. Example of the spectrum for the $4f^7 6s^2\ {}^8S^\circ_{7/2} - y\ {}^8P_{9/2}$ transition in neutral europium-151 and europium-153 at 459.4 nm. The data are in black; the fit is in red. Included are indicators for which transition or crossover is responsible for the spectral feature based of the labels from Fig. 1.

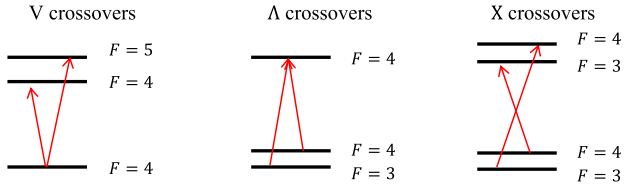

Fig. 5. Three types of crossovers: V crossovers, Λ crossovers, and X crossovers.

with overlapping Doppler profiles, there are, potentially, many crossover features. The three types of crossovers can be seen in Fig. 5. V crossovers are created when the pump and probe beams try to excite the same atoms from the same ground state to different excited states. Λ crossovers and X crossovers occur when the pump beam excites an atom with a particular velocity such that upon decay to a different ground state, that atom has the correct velocity to be excited by the probe beam. A crossover feature appears in a spectrum only when there are atoms in the discharge with the correct velocity to be Doppler shifted into resonance. Both X crossovers and Λ crossovers have negative amplitudes because the pump beam is optically pumping more atoms to a state that is resonant with the probe beam, so there are more atoms for the probe beam to interact with. As such, that feature has a negative amplitude. In all, each isotope has 15 real transitions and up to 62 crossovers. In addition to these three interference crossovers, there could also be collisional crossovers [13]. However, we did not need additional crossovers to fit the spectrum.

The background pressure of the argon gas, the voltage driving the discharge, and the laser power were all studied to determine if any of these systematic effects shift the center of gravity frequencies. For each set of parameters, i.e., pressure, laser power, and discharge current/voltage, a total of eight scans were performed. While checking each possible systematic effect, the other parameters were held constant. For example, while checking the pressure effect, the current driving the discharge was held at −7 mA while the probe and diffracted pump beam saturation parameters were held at 0.6 and 3, respectively. For the pressure effect, spectra were taken at 150 mTorr, 200 mTorr, 250 mTorr, 300 mTorr, and 350 mTorr. For the laser power effect, spectra were taken with probe (pump) saturations of 0.2 (1), 0.4 (2),

0.6 (3), 0.8 (4), and 1 (5). For the voltage effect, the power supply was run in constant voltage mode with voltages of −225 V, −250 V, −275 V, −300 V, and −325 V. In all, a total of 120 scans were taken to study these possible systematic effects.

A. Data Analysis

Given the complex spectrum and large number of possible spectral features, the following methodology is used to determine which features to keep in the fitting and which to drop. To begin, the previously measured hyperfine coefficients and isotope shifts were used to identify an isolated spectral feature. The two isolated features, along with their widths as a function of pressure, can be seen in Fig. 6. The $F = 6 \rightarrow F' = 7$ transition for europium-151 [Fig. 6(C)], was not fully isolated, but could still be fit using data between 2700 MHz and 2820 MHz to extract the FWHM [Fig. 6(D)]. Using Eq. (2), the fitted peak of this spectral feature, and the previously measured hyperfine coefficients and isotope shift [10,11], an initial guess for all possible spectral features and both center of gravity frequencies can be made.

This gives predictions about the position of all possible spectral features. However, it was seen that these predictions began to drift to higher frequencies compared to the actual spectral features indicating a possible small frequency calibration error from the 1978 paper. Therefore, the initial predictions were redone for the europium-151 isotope.

With the initial positions estimated, the spectrum was analyzed to determine if a particular spectral feature was present in the spectrum. Reasons that a possible spectral feature is absent includes weak relative intensities, a feature that would require a large Doppler shift, or an X crossover feature resulting from a single velocity class. If there was a borderline scenario, the fittings were done twice: one fit including the line and one without. Typically, including these borderline scenarios introduced large uncertainties in the fit parameters for those lines and did not change the answer for the hyperfine coefficients or center of gravity. If this was found to be the case, the line was omitted from the final fittings.

After analyzing all possible spectral features, 42 out of a possible 154 transitions and crossovers were used for the final fittings. Very few of the spectral features are well isolated. For much of the spectrum, a positive amplitude spectral feature is near a negative amplitude spectral feature giving the appearance of a derivative "S" shaped signal. It should be emphasized that there are no derivative features in the spectrum; the spectrum is produced using amplitude modulation.

Once the initial guesses had been determined, the entire spectrum was fit using Mathematica's NonlinearModelFit function assuming the ground state hyperfine constants were known and by using the previously measured excited state hyperfine coefficients [11] as initial guesses. The initial guesses for the center of gravity frequencies were those determined using the method described above.

The spectrum also indicates a Gaussian pedestal on many of the spectral features. Referring to Fig. 4, this is most evident on the features near 4200 MHz, 5500 MHz, and 6500 MHz. This background pedestal got smaller as the argon pressure was reduced, which indicates the presence of velocity changing

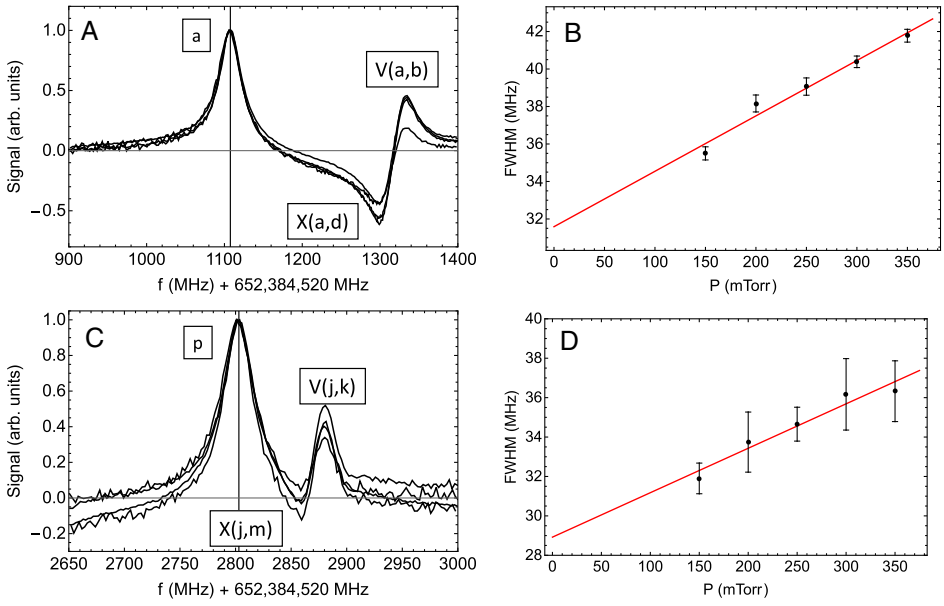

Fig. 6. (A) Example spectrum for the europium-153 $F = 6 \rightarrow F' = 7$ (a) transition, $F = 6 \rightarrow F' = 7$ probe, $F = 5 \rightarrow F' = 6$ pump $X(a, d)$ crossover, and $F = 6 \rightarrow F' = 6/7 V(a, b)$ crossover from four different data sets. The spectra have been normalized for visual purposes. The data sets are (1) $P = 350$ mTorr, $I = -7$ mA, $V = -168$ V, $s_{\text{pump}} = 3$, $s_{\text{probe}} = 0.6$; (2) $P = 200$ mTorr, $I = -7$ mA, $V = -250$ V, $s_{\text{pump}} = 3$, $s_{\text{probe}} = 0.6$; (3) $P = 200$ mTorr, $I = -7$ mA, $V = -250$ V, $s_{\text{pump}} = 2$, $s_{\text{probe}} = 0.4$; (4) $P = 200$ mTorr, $I = -9.6$ mA, $V = -325$ V, $s_{\text{pump}} = 3$, $s_{\text{probe}} = 0.6$. (B) FWHM of the europium-153 $F = 6 \rightarrow F' = 7$ (a) spectral feature as a function of pressure. The laser saturations are $s_{\text{pump}} = 3$ and $s_{\text{probe}} = 0.6$ and the current is −7 mA. The voltage varies with pressure between −330 V and −168 V. The natural linewidth of this transition is $2\pi \times 25.6$ MHz [18]. (C) Example spectrum for the europium-151 $F = 6 \rightarrow F' = 7$ (p) transition, europium-153 $F = 3 \rightarrow F' = 4$ probe, $F = 2 \rightarrow F' = 3$ pump $X(j, m)$ crossover, and europium-153 $F = 3 \rightarrow F' = 3/4 V(j, k)$ crossover from the same four data sets. (D) FWHM of the europium-151 $F = 6 \rightarrow F' = 7$ (p) spectral feature as a function of pressure.

collisions [15]. Given this background, the spectrum was fit to a sum of Lorentzian functions and Gaussian functions:

$$s(f) = \sum_i \frac{A_{L,i}}{1 + \frac{4(f-f_i)^2}{\gamma_i^2}} + A_{G,i} e^{-\frac{(f-f_i)^2}{2\sigma_i^2}},$$

$$f_i = n_1 A_{gs} + n_2 B_{gs} + n_3 A_{es} + n_4 B_{es} + f_{\mathrm{cog}},$$

where n_1, n_2, n_3, and n_4 are fractions determined from Eq. (2), A_{gs} and B_{gs} are the hyperfine coefficients for the ground state for a particular isotope, A_{es} and B_{es} are the hyperfine coefficients for the $y\ ^8P_{9/2}$ state for a particular isotope, $A_{L,i}$ is the amplitude of a spectral feature, $A_{G,i}$ is the amplitude of the Gaussian pedestal, γ_i is the width of a spectral feature, and σ_i is the width of the Gaussian pedestal.

Figure 4 shows an example of a fitted spectrum with residuals. All 120 scans were fit individually to extract the $y\ ^8P_{9/2}$ hyperfine coefficients and center of gravity frequencies for both isotopes with uncertainties. During data collection, alternating scans of linearly increasing laser frequency (scan up) and linearly decreasing laser frequency (scan down) were taken to check for hysteresis effects. For the center of gravity frequencies, a small hysteresis effect of less than 1 MHz was seen between scan up and scan down. To account for this effect, the center of gravity frequency result for a scan up is averaged with the following scan down result. The uncertainty of this average is taken to be the sum of the individual fit uncertainties. As expected, no hysteresis effects were seen with the hyperfine coefficients.

As mentioned above, the argon discharge pressure, the voltage driving the discharge, and laser power were all varied to look for systematic shifts. A small pressure shift was seen in the center of gravity frequencies. The difference between the center of gravity frequencies for the two isotopes showed no statistical pressure dependence indicating both isotopes experienced a similar shift with background pressure. Figure 7 shows the results of the pressure systematic study. Mathematica's NonlinearModelFit function was used to linearly extrapolate the center of gravity frequencies, with uncertainties, to zero pressure. The error bar for each data point is the standard deviation of the fits at that pressure, and these uncertainties were used to weight the linear fitting.

Table 1 shows the final results of this spectral analysis. The uncertainties for the hyperfine coefficients are the standard deviations of the fit results for all 120 scans. The uncertainties for the center of gravity frequencies are the zero pressure extrapolations, which include the statistical uncertainties from the scans, pump/probe parallelism, and the uncertainty on the laser frequency. The uncertainties on the zero pressure extrapolation are 480 kHz and 320 kHz for the europium-153 and europium-151 isotopes, respectively. The pump and probe beams overlap for about 1 m, resulting in a pump/probe parallel uncertainty of 0.5 mRad, which leads to an absolute frequency uncertainty of less than 100 kHz [16]. The uncertainty on the laser frequency is less than 3 kHz. These uncertainties are added in quadrature to give the final uncertainties on the center of gravity frequencies given in Table 1. These uncertainties are summarized in Table 2.

Table 1. Final Results for the Spectral Analysis of the $y\ ^8P_{9/2}$ State

	This Work	From Ref. [11]
A(151) MHz	−228.84(2)	−228.9(2)
B(151) MHz	226.9(5)	226(4)
A(153) MHz	−101.87(6)	−102.4(2)
B(153) MHz	575.4(1.5)	575(8)
f_{cog} (151) MHz	652,389,757.16(34)	
f_{cog} (153) MHz	652,386,593.2(5)	
Isotope shift MHz	3163.8(6)	3111(2)

Table 2. Error Budget for the Center of Gravity Frequencies

	Eu-151	Eu-153
Pressure shift	320 kHz	480 kHz
Pump/probe parallelism	100 kHz	100 kHz
Laser frequency	3 kHz	3 kHz
Overall (quadrature sum)	340 kHz	500 kHz

The centers of gravity for the two stable isotopes agree well with the Doppler broadened spectra obtained by Smith and Tomkins, whose Doppler broadened spectrum had a center value of 652, 387, 360 ± 600 MHz and a width of 6000 MHz [2]. There is a slight disagreement with previously published results for the magnetic dipole hyperfine constant for europium-153 and the isotope shift between the two isotopes [11].

4. CONCLUSION AND FUTURE WORK

This paper reports the first measurement of the center of gravity frequency for the $4f^7 6s^2\ ^8S^\circ_{7/2} - 4f^7(^8S^\circ)6s6p(^1P^\circ)\ ^8P_{9/2}$ transition in neutral europium-151 and europium-153 at 459.4 nm. The fitted hyperfine constants for the excited state are in good agreement with previously published results, with a small discrepancy in the magnetic dipole hyperfine constant for europium-153. This work also finds a discrepancy in the isotope shift measurement.

While there were a large number of possible spectral features, a number of these features were not visible in the spectrum due

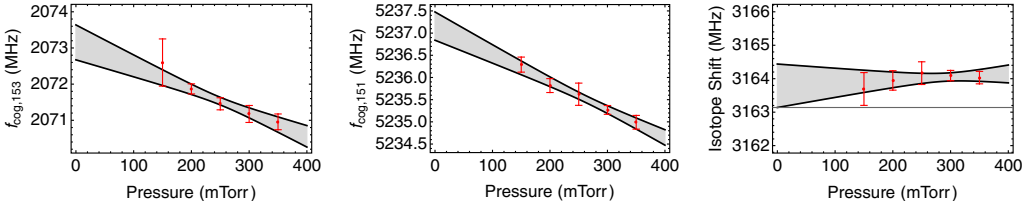

Fig. 7. Pressure shifts for the center of gravity frequencies of (A) europium-153 and (B) europium-151. (C) Isotope shift between the two isotopes.

to weak coupling between some of the hyperfine states and the large hyperfine splittings of the excited state, which minimizes the Doppler profile overlap. Further reduction in the number of crossover features, and thus a possible improvement in the statistical results, can be obtained by performing crossover free saturated absorption spectroscopy [17], by cooling the hollow cathode lamp to reduce the Doppler width of the individual transitions, or by performing the spectroscopy on a well-collimated atomic beam of europium.

Funding. Directorate for Mathematical and Physical Sciences (PHY-1555232, PHY-2110311).

Acknowledgment. The authors thank Ibrahim Sulai of Bucknell University for sharing his design for the hollow cathode lamp and for discussions on fitting, and Dale Renfrow from the Smith College Center for Design and Fabrication for building the lamp. This paper is the result of a course-based research program designed for first year college students (freshmen); the authors thank the Smith College Office of the Provost and Dean of Faculty for personnel support to make this class possible. Finally, the authors thank Timothy Malacarne of Nevada State College and Patricia DiBartolo of Smith College for pedagogical discussions when designing this class.

Disclosures. The authors declare no conflicts of interest.

Data availability. Data underlying the results presented in this paper are not publicly available at this time but may be obtained from the authors upon request.

REFERENCES

1. H. N. Russell and A. S. King, "The arc spectrum of europium," Astrophys. J. **90**, 155 (1939).
2. G. Smith and F. Tomkins, "Absorption spectroscopy of laser excited europium vapour," Proc. R. Soc. Lond. A **387**, 389–406 (1983).
3. B. Furmann, M. Chomski, M. Suski, S. Wilman, and D. Stefańska, "Investigations of the hyperfine structure and isotope shifts in the even-parity level system of atomic europium," J. Quant. Spectrosc. Radiat. Transfer **251**, 107070 (2020).
4. Y. Miyazawa, R. Inoue, K. Nishida, T. Hosoya, and M. Kozuma, "Measuring the branching ratios from the y8P9/2 state to metastable states in europium," Opt. Commun. **392**, 171–174 (2017).
5. R. Inoue, Y. Miyazawa, and M. Kozuma, "Magneto-optical trapping of optically pumped metastable europium," Phys. Rev. A **97**, 061607 (2018).
6. Y. Miyazawa, R. Inoue, H. Matsui, K. Takanashi, and M. Kozuma, "Narrow-line magneto-optical trap for europium," Phys. Rev. A **103**, 053122 (2021).
7. H. Matsui, Y. Miyazawa, R. Inoue, and M. Kozuma, "Understanding one-body losses in magnetically trapped metastable europium atoms," Opt. Commun. **502**, 127408 (2022).
8. Y. Miyazawa, R. Inoue, H. Matsui, G. Nomura, and M. Kozuma, "Bose-Einstein condensation of europium," arXiv:2207.11692 (2022).
9. S. Li, U. N. Le, and H. Saito, "Long-lifetime supersolid in a two-component dipolar Bose-Einstein condensate," Phys. Rev. A **105**, L061302 (2022).
10. P. G. H. Sandars and G. K. Woodgate, "Hyperfine structure in the ground state of the stable isotopes of europium," Proc. R. Soc. Lond. A **257**, 269–276 (1960).
11. G. J. Zaal, W. T. Hogervorst, E. R. Eliel, K. van Leeuwen, and J. Blok, "A high resolution study of the transitions $4f^7 6s^2 \rightarrow 4f^7 6s6p$ in the eu i-spectrum," Zeitschrift für Physik A **290**, 339–344 (1979).
12. E. A. Donley, T. P. Heavner, F. Levi, M. O. Tataw, and S. R. Jefferts, "Double-pass acousto-optic modulator system," Rev. Sci. Instrum. **76**, 063112 (2005).
13. I. A. Sulai and P. Mueller, "Laser spectroscopy of metastable palladium at 340 and 363 nm," Phys. Rev. A **102**, 042805 (2020).
14. V. K. Saini, P. Kumar, K. K. Sarangpani, S. K. Dixit, and S. V. Nakhe, "Development of a see-through hollow cathode discharge lamp for (Li/Ne) optogalvanic studies," Rev. Sci. Instrum. **88**, 093101 (2017).
15. J. Tenenbaum, E. Miron, S. Lavi, J. Liran, M. Strauss, J. Oreg, and G. Erez, "Velocity changing collisions in saturation absorption of u," J. Phys. B **16**, 4543–4553 (1983).
16. S. E. Park, H. S. Lee, T. Y. Kwon, and H. Cho, "Dispersion-like signals in velocity-selective saturated-absorption spectroscopy," Opt. Commun. **192**, 49–55 (2001).
17. A. Banerjee and V. Natarajan, "Saturated-absorption spectroscopy: eliminating crossover resonances by use of copropagating beams," Opt. Lett. **28**, 1912–1914 (2003).
18. N. Penkin and L. Shabanova, "Resonance broadening of europium lines due to a 8s7/2° - y 8p9/2,7/2,5/2 transitions," Opt. Spectrosc. **34**, 368 (1973).